# Seismic Attenuation Imaging of the BAIHETAN Reservoir: Separating Fluids from Fractures in Induced Seismicity


**Yansong Hu[1,2], Luca De Siena[2], Ruifeng Liu[1], Xinjuan He[3], and Lisheng Xu[1]**

[1]Institute of Geophysics, China Earthquake Administration, Beijing, China
[2]Department of Physics and Astronomy "Augusto Righi", Alma Mater Studiorum università di Bologna, Bologna, Italy
[3]Hubei Key Laboratory of Earthquake Early Warning, Institute of Seismology, China Earthquake Administration, Wuhan, China


Sharing is encouraged

This presentation participates in OSPP

Outstanding Student & PhD candidate Presentation contest

ALMA MATER STUDIORUM UNIVERSITÀ DI BOLOGNA

INSTITUTE OF GEOPHYSICS CEA

Institute of Seismology, China Earthquake Administration

## Introduction

Reservoir-induced seismicity is driven by stress changes and pore-pressure variations during water impoundment. The Baihetan reservoir, one of the world's largest hydropower projects, has shown increased seismic activity after impoundment. Previous studies highlight fluid migration along pre-existing faults as a key triggering mechanism. However, distinguishing the roles of fluids and rock fracturing remains challenging. Seismic attenuation is sensitive to both fluid content and fracture density. Here, we use attenuation tomography to image the subsurface beneath the Baihetan reservoir and to separate the effects of fluids and fractures in induced seismicity.

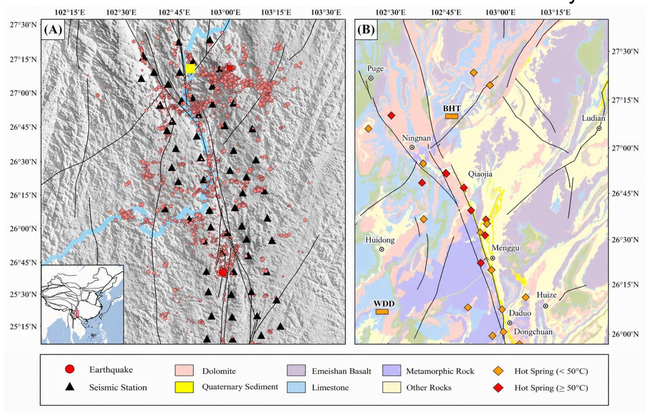


**Figure 1. A:** Seismicity prior to reservoir impoundment and distribution of seismic stations in the study area; **B:** Lithology and hot spring distribution, illustrating the geological framework of the region (Duan et al., 2024)

## Data and Method

Based on the earthquake catalog and relocated dataset of Liu et al. (2023), we used the same seismic events and waveform recordings from the Qiaojia seismic array deployed in the vicinity of the Baihetan reservoir. The dataset covers the period from January 2020 to December 2021 and includes a total of 11,477 relocated earthquakes. Waveform data were quality-controlled, and vertical components were selected to ensure a high signal-to-noise ratio. P- and S-wave arrival times provided in the catalog were used as input for further analysis. Seismic attenuation was imaged using the MuRAT package based on the Coda Normalization (CN) method (Sketsiou et al., 2021) and Peak Delay (PD) method (De Siena et al. 2014). A 3D velocity model from previous studies was adopted for ray tracing during the inversion (Wu et al., 2024) . This approach allows for robust imaging of the 3D attenuation structure, which is sensitive to both fluid content and fracture distribution beneath the Baihetan reservoir.

MuRAT
https://lucadesiena.github.io/MuRAT

Waveform quality control and parameter selection were performed based on time–frequency analysis, as illustrated in Figure 2. Phase arrivals were automatically picked using PhaseNet and visually validated through waveform and spectrogram characteristics. Attenuation measurements were conducted at multiple central frequencies, with a representative example at 6 Hz used to define the coda window and calculate peak delay.

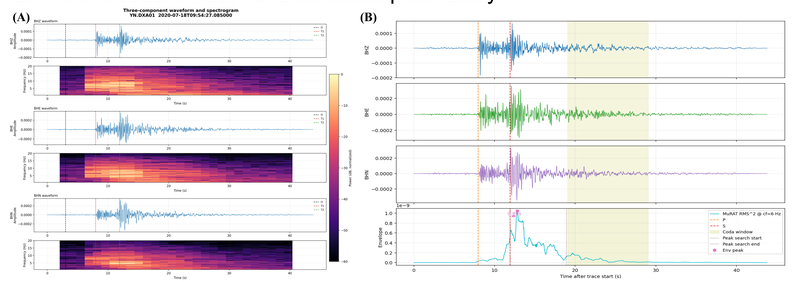


**Figure 2.** Example of waveform quality assessment. **A:** The waveforms and corresponding spectrograms. The spectrograms (0-20 Hz) show clear energy onset after P and S arrivals and typical coda decay; **B:** The coda window starts shortly after S arrival to avoid direct early scatted waves and extends to the end of stable coda. The peak delay is defined as the time difference between the S arrival and the maximum of the envelop within the peak search window.

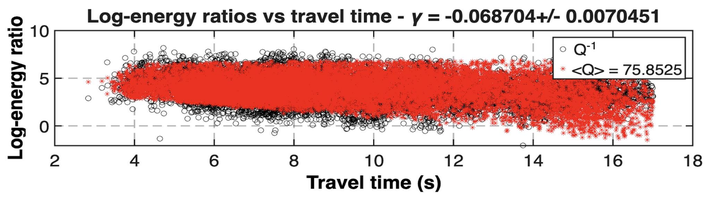


**Figure 3.** The log-energy ratio verses the travel time.

Attenuation was quantified using the Coda Normalization (CN) method. The logarithmic energy ratios decrease approximately linearly with travel time (Figure 3), indicating attenuation effects along seismic ray paths. The slope of the regression line corresponds to $Q^{-1}$, providing a robust estimate of total attenuation (De Siena et al., 2017). The derived attenuation values were subsequently inverted into a 3D attenuation structure, incorporating ray-path.

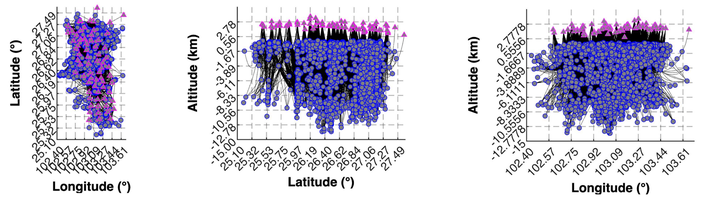


**Figure 4.** Pre-impoundment seismicity and seismic ray coverage of the station network.

## 3D Attenuation Structure

The attenuation images suggest that pre-impoundment seismicity in the Baihetan reservoir area was already influenced by structurally heterogeneous zones. The Qc-anomaly slices show that earthquakes cluster near laterally coherent attenuation anomalies rather than being randomly distributed throughout the model volume. The parameter-separation maps further indicate that many events occur near high-absorption or mixed absorption-scattering domains, whereas the strongest scattering-dominated regions do not systematically host the main earthquake clusters. Overall, these observations suggest that reservoir-area seismicity may be more closely associated with attenuation-sensitive zones than with the most strongly scattering-dominated parts of the model.

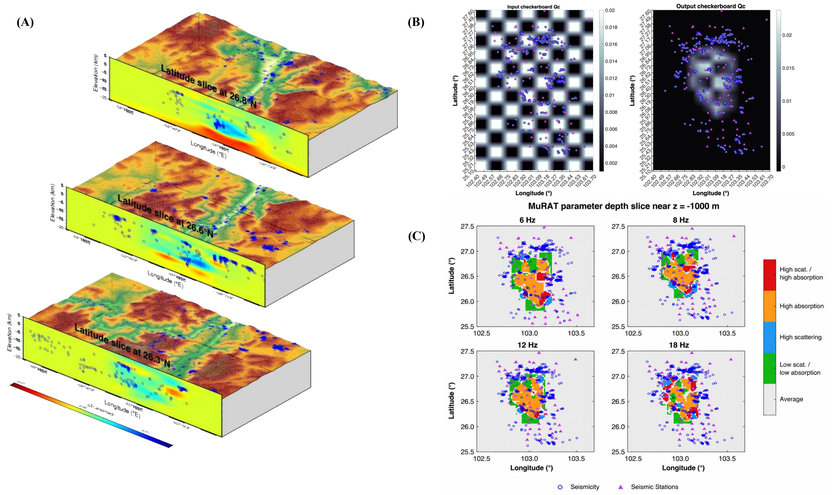


**Figure 5.** Integrated attenuation structure and parameter classification in the Baihetan reservoir area before impoundment. **A:** 3D latitude slices of Qc anomaly, with projected seismicity shown as open blue circles. **B:** checkerboard input and recovered output for Qc, indicating good central resolution. **C:** parameter-separation maps at 6–18 Hz, showing background, scattering-dominated, absorption-dominated, and mixed domains. Seismicity tends to cluster near absorption-dominated or mixed anomalies rather than within the strongest scattering-dominated zones.

## Bibliography


De Siena, L., Thomas, C., & Aster, R. (2014). Multi-scale reasonable attenuation tomography analysis (MuRAT). Journal of Volcanology and Geothermal Research, 277-278, 42-62. https://doi.org/10.1016/j.jvolgeores.2014.03.015

De Siena, L., Amoruso, A., Del Pezzo, E., Wakeford, Z., Castellano, M., & Crescentini, L. (2017). Space-weighted seismic attenuation mapping of Campi Flegrei unrest. Geophysical Research Letters, 44, 1740-1748.

Duan, M., Zhou, L., Zhao, C., & Zhang, X. (2024). Fluid-driven seismicity in the Baihetan reservoir area revealed by 3-D seismic tomography based on dense seismic arrays. Earth and Space Science, 11, e2023EA003397. https://doi.org/10.1029/2023EA003397

Sketsiou, P., De Siena, L., Gabrielli, S., & Napolitano, F. (2021). 3-D attenuation imaging across the Pollino fault network. Geophysical Journal International, 226(1), 536-547. https://doi.org/10.1093/gji/ggab109

Wu, J., Cai, Y., Wang, W., Wang, W., Wang, C., Fang, L., Liu, Y., & Liu, J. (2024). 3-D velocity model at the China Seismic Experimental Site. Science China Earth Sciences, 67(7), 2268-2290. https://doi.org/10.1007/s11430-023-1293-4

Liu, H., Fu, Z., Wu, J. P., Xu, L. S., Zhang, X., Li, C. L., & Li, L. (2023). Seismicity and stress changes before and after Baihetan impoundment. Chinese Journal of Geophysics, 66(10), 4189-4205. https://doi.org/10.6038/cjg2022Q0870